12

Effective Methods for the High Efficiency Dye-Sensitized Solar Cells Based on the Metal Substrates

Ho-Gyeong Yun[1*], Byeong-Soo Bae[2], Yongseok Jun[3] and Man Gu Kang[1]
[1]*Convergence Components & Materials Research Lab., Electronics and Telecommunications Research Institute (ETRI), Daejeon,*
[2]*Lab. of Optical Materials and Coating (LOMC), Dep. of Materials Science and Eng. KAIST, Daejeon*
[3]*Interdisciplinary School of Green Energy, Ulsan National Institute of Science, Ulsan, Republic of Korea*

1. Introduction

A nano porous dye-sensitized solar cell (DSSC) has been widely studied since its origin by O'Regan and Grätzel.[1] By virtue of many sincere attempts, a conversion efficiency of more than 11%[2] and long-term stability[3] has been achieved using a DSSC with F-doped SnO_2 layered glass (FTO-glass). However, relatively low conversion efficiency of the DSSC, compared with the crystalline Si (24.7%) or thin film CIGS (19.9%), restricts its further applications so far.[4] In order to improve the conversion efficiency of the DSSC, continuous attempts have been made in the past decades. Researchers have concentrated their attention on the working or counter electrode materials, synthesizing dye, additives of the electrolytes, nano-structures for enhancing light scattering and so on.[5-9] However, there have been few reports on the interface between nano-crystalline electrode material and current collecting substrates, in particular on the DSSC with thin and light-weight metal substrates. A DSSC with thin and lightweight substrate could extend its application. However, widely used conductive-layer-coated plastic films such as indium doped tin oxide (ITO) coated polyethylene terephthalate (PET) or polyethylene naphthalate (PEN) film degrade at the TiO_2 sintering temperature of approximately 500 ^oC. Furthermore, thermal treatment of TiO_2 particles below plastic degeneration temperature causes poor necking of TiO_2 particles, resulting in a low conversion efficiency.[10] Several methods have been tried in order to answer to this problem, such as hydrothermal crystallization,[11] electrophoretic deposition under high DC fields,[12] and low temperature sintering.[13] However, these methods did not show the fundamental solution for the low necking problem. For better attempts, instead of plastic film, previous study has proposed thin metal foil as a substrates.[14-16] A thin metal foil can be a excellent alternative to conductive-layer-coated plastic films, because temperature limitation due to substrate could be eliminated.

Focusing on the characteristics of the interface between nano-sized TiO_2 and metal substrates, this chapter describes several effective methods for the high efficiency DSSCs

based on metal substrates. Briefly, we report a increased light-to-electricity conversion efficiency and decreased electrical resistance of DSSC with the roughened StSt substrate.[17] In addition, an acid treatment of the Ti substrates for nanocrystalline TiO_2 photo-electrode prior to thermal oxidation significantly improved the optical and electrochemical behaviors at the same time, resulting in a highly increased performance in terms of all performance factors, i.e. V_{oc}, J_{sc}, FF, and efficiency.[18] Finally, a synergistic effect of vertically grown TiO_2 nano tube (TiO_2 NT) array and TiO_2 nano powder (TiO_2 NP) would also be introduced.[19] Detailed experimental procedures are not described in this chapter, because they are well explained in the references.

2. StSt and Ti substrates for photo-electrodes of the DSSCs

Considering the work function of the metals, promising metal substrates for DSSCs are Ti, StSt, tungsten (W) and Zinc (Zn)[14] because the work function determine the contact types, i.e. ohmic contact or schottky contact. In case of the n-type semiconductor such as TiO_2, the work function of the metal should be lower than that of semiconductor, ohmic contact. Furthermore, in the metals such as Ti, StSt, W, and Zn, the oxide layer produced by thermal treatment play important roles in the cell properties.[16] However, during thermal treatment, Al, Co, and etc generate insulating oxide layer, which make it insulator. Ti is most desirable metal substrate of the DSSCs because the thermally oxidized layer might have very similar structure with the nano-crystalline TiO_2 layer. The almost same electrochemical impedance of the W with the Ti was also reported. Under the assumption that most of the oxide layer is WO_3, the conduction band energy level of the W locates only 0.15 V below the one of TiO_2, as shown in Fig. 1[16] When the mutual disposition of energy levels is considered, the conduction band energy levels of the facing semiconductor metal oxides overlap.[20, 21] This overlapping does not significantly block the charge carriers flow, and no noticeable increase of the resistance has been reported.[16] However, W is not a common but rare metal. In the case of the StSt, some higher electrochemical impedance than Ti was reported due to conduction band energy level mismatch. However, StSt is most common and cost-effective material for the substrates of the DSSCs. Therefore, Ti and StSt are most frequently focused at the realization of the DSSCs on the metal substrates.[22-26]

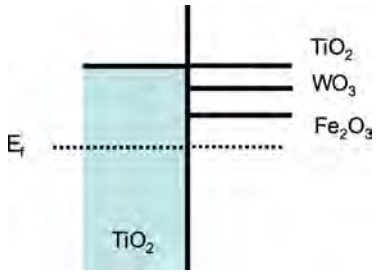

Fig. 1. Diagram of the conduction band edges of the semiconductor metal oxides. © The Electrochemical Society[16].

3. StSt substrate: effect of increased surface area[17]

The injection process used in the DSSC does not introduce a hole, i.e. minority carriers, in the TiO_2, only an extra electron.[27] On the contrary, as majority carriers and minority

carriers, electrons and holes co-exist in *p-n* junction type solar cell, causing high electron/hole recombination rate. Therefore, in order to decrease the emitter recombination as much as possible, point-contact solar cells were introduced.[28, 29] In this paragraph, however, we report increased conversion efficiency and decreased electrical resistance of DSSCs with the roughened StSt substrates. Sulfuric acid-based solutions are effective StSt pickling reagents.[30] Additives, such as hydrated sodium thiosulphate and propargyl alcohol, endowed the StSt with pores and increased the surface area.[31] Under the atomic force microscope (AFM) analysis, the actual surface area of the roughened StSt substrates were measured to be a 23.6% increase. (Fig. 2)

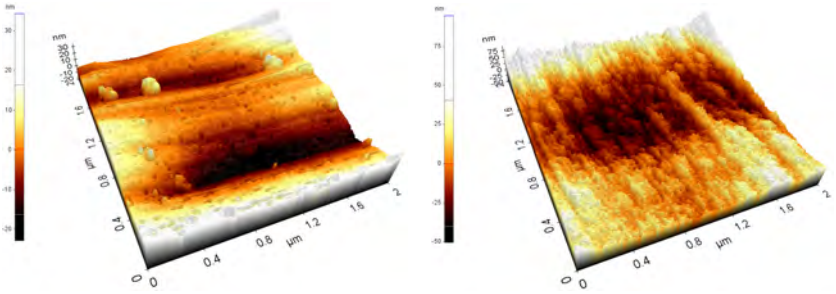

(a) (b)

Fig. 2. AFM images of StSt surface (a) before and (b) after roughening process. © American Institute of Physics[17].

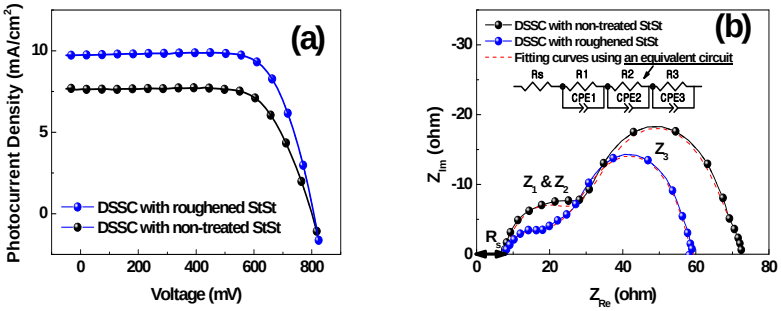

Fig. 3. Under AM 1.5 irradiation (100 mW/cm²) with a xenon lamp. (a) *J-V* curves of DSSC with nontreated StSt substrates and roughened StSt substrates. (b) Electrochemical impedance spectra measured at the frequency range of 10^{-1}–10^{6} Hz and fitting curves using an equivalent circuit model including three CPEs. © American Institute of Physics[17].

The *J-V* characteristics of the DSSCs with non-treated and roughened StSt substrates are shown in Fig. 3. (a). After roughening, the conversion efficiency and J_{sc} of the DSSC increased 33% and 27% respectively. However, open circuit voltage (V_{oc}) and fill factor (*FF*) remained nearly constant. V_{oc} changed from 800 mV to 807 mV and *FF* varied from 70.3% to 72.4% after roughening. To identify the cause of the increased J_{sc} and efficiency, electrochemical impedance spectra were measured in the frequency range of 10^{-1} to 10^{6} Hz

and the resistance from electrochemical impedance spectra was estimated using the equivalent circuit model including 3 constant phase elements (CPEs). (Fig. 3. (b)) Even though there were small differences in R_2 and R_3 after roughening, R_1 was reduced from 17.1 to 3.9. The largely reduced R_1 clearly comes from the reduced electrical resistance of the TiO_2/StSt interface because R_1 represents the electrical resistance at this interface.[32] Considering the same electrical resistance between the TiO_2 particles and the interface with the Pt/electrolyte in DSSCs with both non-treated and roughened substrates, the small difference of R_2 after roughening is expected result. The value of R_3 is closely related to the reverse electron transfer from TiO_2 to the electrolyte.[32] In detail, as the number of electrons returning to the electrolyte increases, the arc of Z_3 increases. Therefore, the fact that R_3 remains unchanged after roughening clearly indicates that the increased electrical contact area does not cause an increase in reverse electron transfer.

4. Ti substrate: a simple surface treating method[18]

In this paragraph, we report that acid (HNO_3-HF) treatment of the titanium (Ti) substrate for the photo-electrode significantly improved the efficiency of DSSCs. Prior to spreading the TiO_2 paste, the Ti substrates were chemically treated with HNO_3-HF solution. As shown in Fig. 4 (a) and (b), HNO_3-HF treatment caused sharp steps at the grain boundaries, due to different etching rates of dissimilar crystal structures between the grains and the grain boundaries.[33] Fig. 5 (a) ~ (c) shows the cross-sectional scanning transmission electron microscopy (STEM) images of the Ti substrates. On the outermost surface, the non-treated Ti substrate exhibited a finer-grained structure. This suggests that the outermost surface of the Ti substrate was composed of finer-grained disordered Ti, which resulted from the thermo-mechanical manufacturing process.[34] However, treatment of the Ti substrate with the HNO_3-HF solution completely removed this finer-grained disordered region. Furthermore, the thermally oxidized layer of the non-treated substrate was much thicker and more variable than that of the HNO_3-HF-treated substrates. (Fig. 5 and 6) In the field emission transmission electron microscope (FE-TEM) analysis, the oxidized layer of the non-treated Ti substrate, which was produced by oxygen diffusion to the finer-grained disordered region, showed a disordered grain structure, i.e. a low degree of crystallinity. However, the oxide layer of HNO_3-HF-treated Ti substrates, which was developed by the oxygen diffusion into the normally-grained Ti substrate, was almost a single crystal. The corresponding X-ray diffraction (XRD) patterns also showed that the HNO_3-HF treatment had produced a variation on the phase and crystallinity of a thermally oxidized layer.

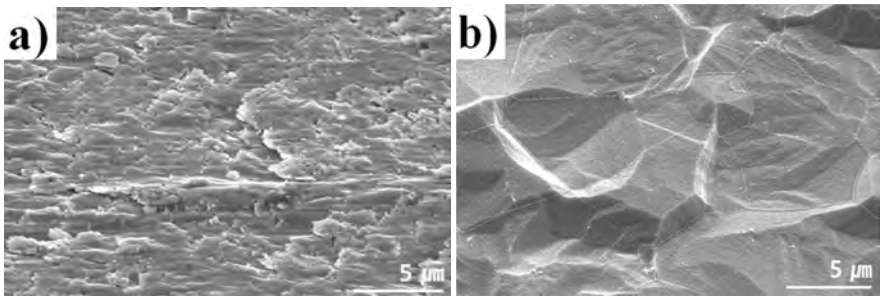

Fig. 4. SEM images of the Ti surface before thermal annealing: (a) non-treated, (b) HF-HNO3 treated. © WILEY-VCH Verlag GmbH & Co. KGaA, Weinheim[18].

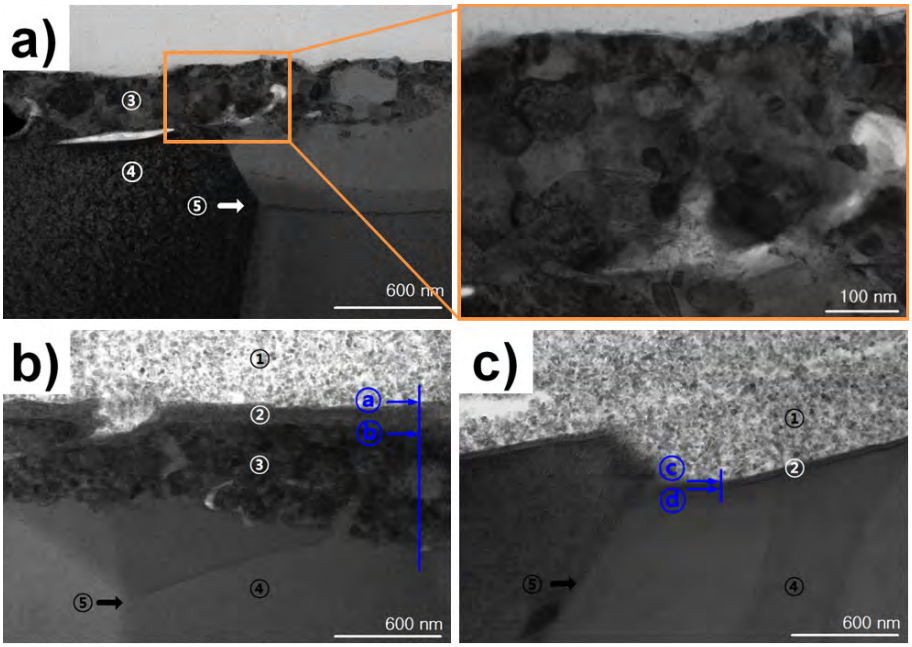

Fig. 5. Cross-sectional STEM images of Ti substrates (a) untreated substrate before thermal annealing, including a magnified view of the finer grained disordered region, (b) untreated substrate after thermal annealing at 550 °C for 30 min, (c) HF-HNO_3-treated substrate after thermal annealing. Note: ① sintered TiO_2 particles, ② thermally oxidized Ti, ③ finer-grained disordered Ti, ④ normally grained Ti, ⑤ normal grain-boundaries of Ti. © WILEY-VCH Verlag GmbH & Co. KGaA, Weinheim[18].

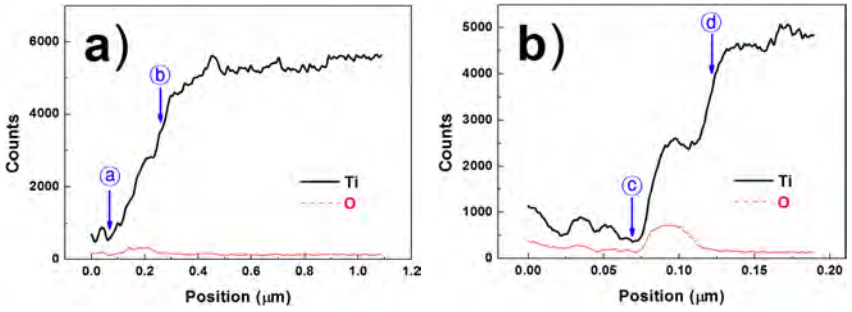

Fig. 6. EDX graph of (a) a line-scan shown in Fig. 5 (b), (b) a line-scan shown in Fig. 5 (c). © WILEY-VCH Verlag GmbH & Co. KGaA, Weinheim[18].

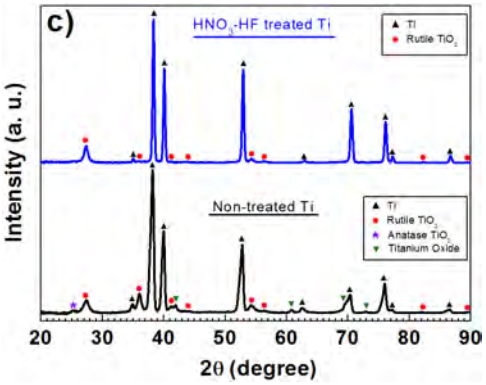

Fig. 7. By use of a 2θ scan method, XRD patterns of non-treated and HNO_3-HF-treated Ti substrates after thermal annealing at 550 °C for 30 min. © WILEY-VCH Verlag GmbH & Co. KGaA, Weinheim[18].

As shown in Fig. 7, the thermally oxidized layer of the non-treated Ti substrate exhibited various oxide forms including anatase TiO_2, rutile TiO_2, and titanium oxide. However, only rutile TiO_2 was observed in the oxide layer of the HNO_3-HF-treated Ti substrate.
The variation of the microstructures influenced the optical and electrochemical behaviour at the same time resulting in highly increased efficiency, 9.20%. (Fig. 8 (d)) Fig. 8 (a) shows the optical reflection of the Ti. The HNO_3-HF-treated substrate exhibited a significantly increased optical reflection. The low and flat reflection behavior of the non-treated Ti substrates could be attributed to the thick and non-uniform thickness of the oxide layer and the inferior optical reflectance at the inner metal surface.[35, 36] In the evaluation of the illumination intensity effect on the performance factors, the V_{oc} and J_{sc} exhibited logarithmic and linear dependence respectively. However, *FF* decreased under stronger illumination intensity. These consequences suggest that the improved performance of the DSSC with the HNO_3-HF-treated substrate cannot be attributed to the enhanced optical reflection alone. Rather, the greater part of this improvement could be attributed to a reduced back reaction of the electrons with I_3^- ions at the interface of the conductive substrate and electrolyte because the thickness of the nano crystalline TiO_2 layer is about 15㎛. For a device with a > 10 ㎛ thick TiO_2 layer, performance increases due to reflection are restricted to wavelengths above 580 nm where the absorption of the N719 dye is weak.[15]
The blocking layer (compact TiO_2) at the interface of the TiO_2 particles/conductive substrates has been studied[37, 38] and several groups concluded that recombination occurs predominantly near the conductive substrate and not across the entire TiO_2 film.[39] In the DSSCs with metal substrates, the oxidized layer is naturally formed at the interface of the TiO_2 particles/conductive substrate during thermal annealing. However, it seems that the low quality oxidized layer induced poor blocking behavior of the DSSCs with the non-treated Ti substrates. The recombination kinetics were investigated by the evaluation of the rate of photovoltage decay. The rate of photovoltage decay is inversely proportional to the lifetime of the photoelectron in the DSSCs, and the lifetime of the electron is inversely proportional to the rate of recombination.[40] The HNO_3-HF treatment of the Ti substrates strongly influenced the rate of the photovoltage decay. (Fig. 8 (b)) The electron recombination may lead to a lowering of the photocurrent, but also to a decrease in the

photovoltage by lowering the quasi-Fermi level for the electrons under illumination due to a kinetic argument.[41, 42] Furthermore, the *FF* is a measure of the increase in recombination (decrease in photocurrent) with increasing photovoltage.[43] If the improved optical reflection at the substrate were a dominant element of enhanced performance, the V_{oc} and *FF* would restrictively increase and decrease respectively. An obviously possible cause for the significantly improved performance is decreased recombination at the interface of the TiO_2/conductive substrate after HNO_3-HF treatment.

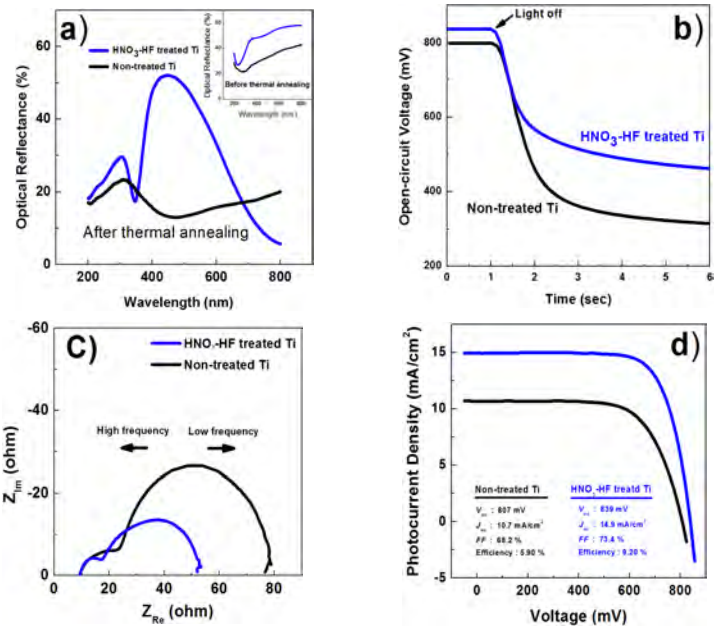

Fig. 8. (a) Optical reflectance of Ti substrates measured with UV-VIS-NIR spectro-photometers combined with an integrated sphere before and after thermal annealing at 550 °C for 30 min. Baseline calibration was performed with a standard specimen composed of polytetrafluoroethylene (PTFE). (b) open-circuit voltage decay measurement, (c) electrochemical impedance spectra, and (d) J-V curves of DSSC with non-treated and HNO_3-HF-treated Ti substrates. © WILEY-VCH Verlag GmbH & Co. KGaA, Weinheim[18].

As shown in Fig. 8 (c), electrochemical impedance also improved after HNO_3-HF treatment. The 1st semicircle is closely related to charge transfer at the counter electrode and/or electrical contact between conductive substrate/TiO_2 or TiO_2 particles.[22] The relatively small size of the 1st semicircles (high frequency range) in the cell with the HNO_3-HF-treated substrate indicated a reduced electrical resistance, i.e. improved contact at the TiO_2/Ti interface accordingly. Furthermore, the size of the 2nd semicircle (low frequency range) was also largely decreased. The 2nd semicircle is related to the recombination of electrons with I_3^-.[14] Under the assumption that the micro-structures of the oxidized layers determine the blocking ability, the significantly decreased size of the 2nd semicircle could be attributed to a highly decreased charge recombination by virtue of improved micro-structure after HNO_3-HF treatment of the Ti substrate.

5. Hybrid substrate: TiO_2 NP on the TiO_2 NT grown Ti substrates[19]

In the case of DSSCs based on metal substrates, light illumination should come from a counter electrode, i.e., back illumination. Therefore, the light scattering layer,[9] which enhances the optical path length, should be located between 20 nm sized TiO_2 nano-particles (NPs) and conductive substrates. This structure causes poor adhesion due to the large particle size of the scattering layer. Considering slow recombination and light scattering,[44] TiO_2 nano-particles has been incorporated on the short TiO_2 nano-tube grown Ti substrates. The preparation of photo-electrode is completed by four steps: ① anodization of a Ti foil for the formation of short TiO_2 NT arrays, ② doctor blading of TiO_2 NP included paste on the TiO_2 NT formed Ti substrates, ③ thermal treatment of the photo-electrode prepared by step ① & ②, ④ dye coating. In our approach, therefore, the fabrication time and length of TiO_2 NT could be minimized without diminishing, rather increasing, the surface area of the photo-electrode.

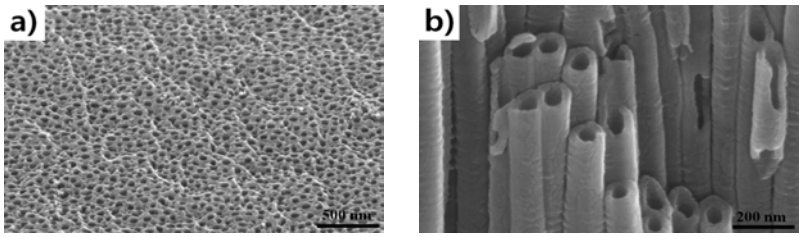

Fig. 9. SEM images of the TiO_2 NT fabricated Ti for 30 min anodizing (a) surface and (b) cross-section. © The Royal Society of Chemistry[19].

Out of several fabrication method of the TiO_2 NT such as electrochemical anodizing,[45] hydrothermal synthesis,[46] and template-assisted synthesis,[47] anodizing is a relatively simple approach for the preparation of optimized TiO_2 NT.[48] Anodizing at 50 V in a solution of ethylene glycol containing ammonium fluoride (NH_4F) resulted in the formation of regular TiO_2 NT arrays. (Fig. 9) When the anodizing was performed for 30 min, the tube diameter and wall thickness were estimated to be about 100 and < 50 nm, respectively. The lengths of the TiO_2 NT layers were controlled by the anodizing time. When the anodizing was performed for 15, 30, and 60 min, the lengths of the TiO_2 NTs were 1.53, 4.36, and 8.17 μm, respectively. TiO_2 NT and TiO_2 NP bonded well following thermal annealing at 550 °C for 30 min. (Fig. 10)

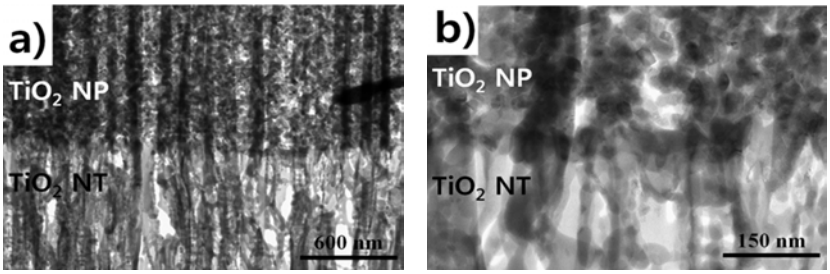

Fig. 10. Cross-sectional TEM images of (a) interface between TiO_2 NP and TiO_2 NT (b) magnified view of (a). © The Royal Society of Chemistry[19].

As is same with the previous paragraph, the TiO_2 NP film was made 15 μm thick, because that was the size that allowed DSSCs to exhibit optimal performance. When the thickness of the TiO_2 NP was more than 15 μm, the DSSC with TiO_2 NP on the Ti substrate (TiO_2 NP/Ti) exhibited a lowered performance because the thick TiO_2 layer (> 15 μm) provided additional electron recombination sites, resulting in a decreased open-circuit voltage (V_{oc}) and fill factor (*FF*).[49] However, a performance of the DSSCs with TiO_2 NP+NT/Ti increased continuously with increasing TiO_2 NT thickness up to 30 min anodized TiO_2 NT. (Fig. 11 (a)) This difference between the DSSC with TiO_2 NP+NT/Ti and the DSSC with TiO_2 NP/Ti can be attributed to the TiO_2 NT having an electron recombination that was reduced by comparison with the TiO_2 NP. The electron lifetime in the TiO_2 NT was longer than that in the TiO_2 NP because of the electron-recombination suppression from the reduction in electron-hopping across the inter-crystalline contacts between the grain boundaries.[50] As is described in the previous paragraph, optical transmission is restricted to wavelengths > 570 nm for a device with a TiO_2 layer that is more than 10 μm thick, resulting in a restricted increase in J_{sc}.[15] However, strong internal light scattering within the TiO_2 NTs elongated the path length of the long-wavelength incident light to promote the capture of photons by the dye molecules.[44] Despite a surface area of the DSSC with TiO_2 NP on 30-min-anodized TiO_2 NT/Ti that was smaller than that of DSSC with 20 ㎛ thick TiO_2 NP/Ti, the increased J_{sc} could also be a result of stronger light scattering effects.

The reduced electron recombination at the interface of the TiO_2 NT/electrolyte was also represented in an electrochemical impedance measurement (Fig. 11 (b)). Under the assumption that the TiO_2 NT is superior to TiO_2 NP in the interfacial contact with Ti substrates due to the *in-situ* fabrication process, the largely reduced size of the 1st semicircle in a DSSC with TiO_2 NP+NT/Ti could be a result of the reduced electrical resistance at the interfacial contact. However, the size of the 2nd semicircle (low frequency range) was almost the same. The 2nd semicircle represents the recombination of injected electrons to the TiO_2 film with electrolyte.[51] Furthermore, the DSSCs with TiO_2 NP/Ti and TiO_2 NP+NT/Ti exhibited a similar rate of photovoltage decay, which is proportional to the rate of recombination (Fig. 11 (c)). The overall TiO_2 film in the DSSC with TiO_2 NP+NT/Ti was thicker than that of the DSSC with TiO_2 NP/Ti due to the introduction of the TiO_2 NT layer at the interface of the TiO_2 NP and Ti substrate. Therefore, it seems that the small variation in the 2nd semicircle in the electrochemical impedance spectra and the rate of photovoltage decay can be attributed to the slow recombination characteristics of the TiO_2 NT.

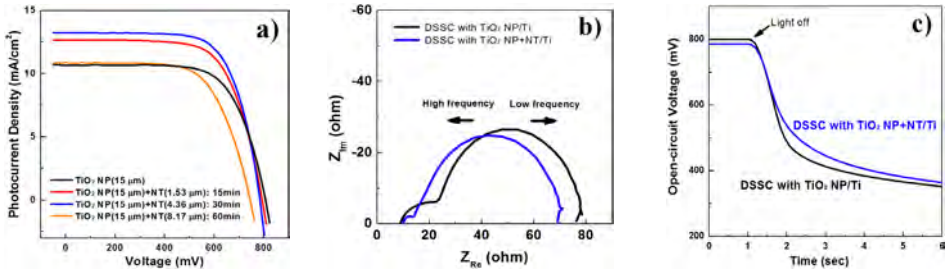

Fig. 11. (a) *J*–*V* characteristics of the DSSC with TiO_2 NP/Ti and TiO_2 NP + NT/Ti. (b) Electrochemical impedance spectra in frequencies ranging from 10^{-1} to 10^6 Hz. (c) Open-circuit voltage decay measurement. © The Royal Society of Chemistry[19].

6. Conclusion

Several methods for the high efficiency DSSCs based on the metal substrates have been introduced. In the case of the StSt substrate, the solar cell performance was significantly improved by the roughening process, which enhances electrical contact by roughening the substrates. In addition, when a Ti substrate was treated with an acid solution, both the surface morphology and the crystalline structure of the thermally oxidized layer were varied, resulting in the simultaneous improvements in V_{oc}, J_{sc} and *FF*. Finally, the DSSCs with TiO_2 NP + NT/Ti were prepared for the synergistic effect of vertically grown TiO_2 NTand TiO_2 NP films. The slow electron recombination at the interface of the TiO_2 NT/electrolyte and the light scattering effect might have simultaneously contributed to DSSC performance, resulting in the improved *Jsc* and conversion efficiency with only a negligible effect on the V_{oc} and *FF*.

7. Acknowledgements

This article is prepared and reproduced under the permission of the American Institute of Physics, WILEY-VCH Verlag GmbH & Co. KGaA, The Electrochemical Society, and The Royal Society of Chemistry. Each article has been referred at the corresponding section.

8. References

[1] B. O'Regan, M. Grätzel, *Nature* 353, 737 (1991)
[2] M. K. Nazeerudden, P. Pechy, T. Renouard, S. M. Zakeeruddin, B. R. Humphry, P. Comte, P. Liska, L. Cevey, E. Costa, V. Shklover, L. Spiccia, G. B. Deacon, C. A. Bignozzi, M. Grätzel, *J. Am. Chem. Soc*. 123, 1613 (2001)
[3] P. Wang, S. M. Zakeeruddin, J. E. Moser, K. Nazeeruddin, T. Sekiguchi, M. Grätzel, *Nat. Mat*. 2, 402 (2003)
[4] M. A. Green, K. Emery, Y. Hishikawa, W. Warta, *Progress in Photovoltaics* 17, 320 (2009)
[5] Y. J. Kim, M. H. Lee, H. J. Kim, G. Lim, Y. S. Choi, N. -G. Park, K. Kim, W. I. Lee, *Adv. Mater*. 21, 3668 (2009)
[6] A. Nattestad, A. J. Mozer, M. K. R. Fischer, Y. –B. Cheng, A. Mishra, P. Bäuerle, U. Bach, *Nature Mater*. 9, 31 (2010)
[7] F. Gao, Y. Wang, J. Zhang, D. Shi, M. Wang, R. Humphry-Baker, P. Wang, S. M. Zakeerudding, M. Grätzel, *Chem. Commun*. 2635 (2008)
[8] M. Wang, X. Li, H. Lin, P. Pechy, S. M. Zakeeruddin, M. Grätzel, *Dalton Trans*. 10015 (2009)
[9] S. Ito, S. M. Zakeeruddin, R. Humphry-Baker, P. Liska, R. Charvet, P. Comte, M. K. Nazeeruddin, P. Péchy, M. Takata, H. Miura, S. Uchida, M. Grätzel, *Adv. Mater*. 18, 1202 (2006)
[10] C. Y. Jiang, X. W. Sun, K. W. Tan, G. Q. Lo, A. K. K. Kyaw, D. L. Kwong, *Appl. Phys. Lett*. 92, 143101 (2008)
[11] D. Zhang, T. Yoshida, H. Minoura, *Adv. Mater*. 15, 814 (2003)
[12] D. Mattews, A. Kay, M. Grätzel, *Aust. J. Chem*. 47, 1869 (1994)
[13] C. Longo, A. F. Nogueira, M. A. De Paoli, H. Cachet, *J. Phys. Chem. B* 106, 5925 (2002)
[14] M. G. Kang, N. G. Park, K. S. Ryu, S. H. Chang, K. J. Kim, *Sol. Energy Mater.Sol. Cells* 90, 574 (2006)

[15] Y. Jun, J. Kim, M. G. Kang, *Sol. Energy Mater. Sol. Cells* 91, 779 (2007)
[16] Y. Jun, M. G. Kang, *J. Electrochem. Soc*. 154, B68 (2007)
[17] H. -G. Yun , Y. Jun , J. Kim , B. -S. Bae , M. G. Kang , *Appl. Phy. Lett*. 93, 133311 (2008)
[18] H. -G. Yun , B. -S. Bae, M. G. Kang , *Advanced Energy Materials* 1, 1 (2011)
[19] H. -G. Yun , J. H. Park , B. -S. Bae , M. G. Kang , *J. Mater. Chem*. 21, 3558 (2011)
[20] M. K. Kang, N. G. Park, S. R. Kwang, H. C. Soon, K. J. Kim, *Chem. Lett.* 34, 804 (2005)
[21] H. H. Kung, H. S. Jarrett, A. W. Sleight, A. Ferretti, *J. Appl. Phys.* 48, 2463 (1977)
[22] J. H. Park, Y. Jun, H. –G. Yun, S. –Y. Lee, M. G. Kang, *J. of Electrochem. Soc.* 155, F145 (2008)
[23] H. Lindström, A. Holmberg, E. Magnusson, S. Lindquist, L. Malmqvist, A. Hagfeldt, *Nano Lett.* 1, 97 (2001)
[24] S. Uchida, M. Tomiha, H. Takizawa, M. Kawaraya, *J. of Photochem. and Photobio. A: Chem* 164, 93 (2004)
[25] T. Miyasaka, Y. Kijitori, *J. of Electrochem. Soc*. 151, A1767 (2004)
[26] M. Dürr, A. Schmid, M. Obermaier, S. Rosselli, A. Yasuda, G. Nells, *Nature Mat.* 4, 607 (2005)
[27] J. N. Hart, Y. -B. Cheng, G. P. Simon, L. Spiccia, *J. of Nanoscience and Nanotech*. 8, 2230 (2008)
[28] T. Markvat, L. Castaner, Solar Cells: Materials, Manufacture and Operation, Elsevier Science, Oxford, 377 (2005)
[29] R. M. Swanson, S. K. Beckwith, R. A. Crane, W. D. Eaides, Y. O. Kwark, R. A. Sinton, S. E. Swiiwiun, *IEEE Trans. on Elec. Dev*. 31, 5 (1984)
[30] A. Tamba, N. Azzerri, *J. App. Electrochem*. 2, 175 (1972)
[31] S. E. Hajjaji, M. E. Alaoui, P. Simon, A. Guenbour, A. Ben Bachir, E. Puech-Costes, M. T. Maurette, L. Aries, *Sci. and Tech. of Adv. Mat*. 6, 519 (2005)
[32] T. Hoshikawa, M. Yamada, R. Kikuchi, K. Eguchi, *J. Electrochem. Soc*. 152, E68 (2005)
[33] J. Lichtscheidl, K. J. Hartig, N. Getoff, C. Tauschnitz, G. Nauer, *Z. Naturforsch. A* 36a , 727 (1981)
[34] P. R. F. Barnes, L. K. Randeniya, P. F. Vohralik, I. C. Plumb, *J. Electrochem. Soc*. 154 , H249 (2007)
[35] G. Jerkiewicz, H. Strzelecki, *Langmuir* 12, 1005 (1996)
[36] J. –L. Delplancke, M. Degrez, A. Fontana, R. Winand, *Surface Tech*. 16 , 153 (1982)
[37] J. Xia, N. Masaki, K. Jiang, S. Yanagida, *Chem. Commun*. 138 (2007)
[38] B. Peng, G. Jungmann, C. Jäger, D. Haarer, H.-W. Schmidt, M. Thelakkat, *Coord. Chem. Rev*. 248, 1479 (2004)
[39] K. Zhu, E. A. Schiff, N. -G. Park, J. V. D. Lagemaat, A. J. Frank, *Appl. Phys. Lett*. 80, 685 (2002)
[40] A. Zaban, M. Greenshtein, J. Bisquetr, *Chem. Phys. Chem* 4, 859 (2003)
[41] Hagfeldt, M. Grätzel, *Chem, Rev*. 95, 49 (1995)
[42] Kumar, P. G. Santangelo, N. S. Lewis, *J. Phys. Chem*. 96, 834 (1992)
[43] D. Cahen, G. Hodes, M. Grätzel, J. F. Guillemoles, I. Riess, *J. Phys. Chem. B* 104, 2053 (2000)
[44] K. Zhu, N. R. Neale, A. Miedaner, A. J. Frank, *Nano Lett*. 7, 69 (2007)
[45] D. Gong, C. A. Grimes, O. K. Varghese, W. C. Hu, R. S. Singh, Z. Chen, E. C. Dickey, *J. Mater. Res*. 16, 3331 (2001)
[46] T. Kasuga, M. Hiramatsu, A. Hoson, T. Sekino, K. Niihara, *Langmuir* 14, 3160 (1998)

[47] P. Hoyer, *Langmuir* 12, 1411 (2006)
[48] G. K. Mor, K. Shankar, M. Paulose, O. K. Varghese, C. A. Grimes, *Nano Lett*. 5, 191 (2005)
[49] R. Kato, A. Furube, A. V. Barzykin, H. Arakawa, M. Tachiya, *Coord. Chem. Rev*. 248, 1195 (2004)
[50] C.-J. Lin, W.-Y. Yu, S.-H. Chien, *Appl. Phys. Lett*. 93, 133107 (2008)
[51] T. Hoshikawa, M. Yamada, R. Kikuchi, K. Eguchi, J. Electrochem. Soc. 152, E68 (2005)